



# **DREAMERS**

Design REsearch, implementation And Monitoring of Emerging technologies for a new generation of Resilient Steel buildings

# Report on the site tests

## **Deliverable D5.2**

WP 5 - Task 5.2: Site tests on the building

## **Coordinator:**

Vincenzo Piluso

#### Authors:

Fabrizio Barone, Marco Casazza, Rosario Montuori, Elide Nastri,
Vincenzo Piluso

University of Salerno, Fisciano (SA), Italy









с .

UNIVERSIDADE DE COIMBRA





MOTT MACDONALD



# **Contents**

LIS	T OF FIGURES	ii
LIS	T OF TABLES	iii
1.	Introduction	1
2.	Description of the seismic sensor and the standalone monitoring solution	1
3.	Measurement setup and sensor placement	3
		3
4.	Signal acquisition and spectral processing	7
5.	Operational modal analysis results 1	1
6.	FEM Modal Analysis 1	3
7.	Conclusions 1	17
8.	References	18

# **LIST OF FIGURES**

Figure 1. Plan positioning of the sensors in the first campaign of October 12, 20244
Figure 2. Sensors 33H and 39H in the lower right corner of the building with reference to Figure 14
Figure 3. Sensors 30H and 35H in the lower right corner of the building with reference to Figure 15
Figure 4. Plan positioning of the sensors in the second campaign of June 07, 20256
Figure 5. Sensors 29H and 35H in the high left corner of the building with reference to Figure 46
Figure 6. Sensors 34H and 33H in the middle of the building with reference to Figure 47
Figure 7. Translational displacement signals recorded during the first campaign in the points of Figure 18
Figure 8. Translational displacement signals recorded during the second campaign in the points of Figure 49
Figure 9. Fourier Density Spectra of the displacement signals recorded in the points of Figure 1 during the first campaign10
Figure 10. Fourier Density Spectra of the displacement signals recorded in the points of Figure 4 during the second campaign11
Figure 11. Modal analysis contours for the FEM simulations of the building in the configuration of the first campaign of October 12, 202414
Figure 12. Modal analysis contours for the FEM simulations of the building in the configuration of the second campaign of June 07, 2025

# **LIST OF TABLES**

Гable 1. Comparison in terms of periods and frequencies between FEM simulations b
SAP2000 and measures with reference to the first campaign of dynamic identificatio
(October 12, 2024)1
Table 2. Comparison in terms of periods and frequencies between FEM simulations b
SAP2000 and measures with reference to the second campaign of dynamic identificatio
(June 07, 2025)1

#### 1. Introduction

Within the framework of the DREAMERS project (Design REsearch, implementation And Monitoring of Emerging technologies for a new generation of Resilient Steel structures), the experimental validation of newly developed anti-seismic technologies plays a central role. Among these, the FREEDAM (Free from Damage) connections — a friction-based solution designed to provide energy dissipation and self-centering capacity without structural damage — have been implemented in a full-scale demonstrator building, known as C3.

To assess the in-situ performance of the FREEDAM system, a campaign of experimental tests has been carried out, as foreseen by Task 5.2. The main objective was the dynamic identification of the structure, allowing for the estimation of natural frequencies, vibration modes, and equivalent damping ratios. These parameters are essential for validating the finite element models developed in earlier work packages (notably WP2 and WP4), which were used also for blind predictions in coordination with UNINA.

Two monitoring campaigns were conducted at different stages of the building's construction:

- The first on October 12, 2024, when the building was in an intermediate construction state, with the steel frames, composite floor slabs, and staircase core completed, but without any nonstructural or finishing elements;
- The second on June 7, 2025, when the building was nearly completed, with façades, partitions, services, and roof installations in place.

Contrary to what was originally foreseen in Task 5.2, no traditional dynamic testing equipment was used. Such a traditional set up typically includes a vibrating machine (i.e., a vibrodyne), used to produce an artificial vibration input, in combination with a set of accelerometers, employed for the measure. Instead, due to the need for a higher-sensitivity characterization, an innovative solution was adopted, reflecting the experimental character of the C3 demonstrator. The building, being a world-first implementation of FREEDAM technology at real scale, deserved a non-invasive and high-resolution vibration monitoring solution, typically used in advanced applications such as gravitational wave detection and precision dynamics.

The monitoring setup relied on monolithic broadband high-sensitivity seismometers, specifically designed to measure displacement in the low-frequency range with excellent signal-to-noise ratio. Installed in a standalone configuration and based on an open-loop sensing principle, this system enabled output-only modal identification, avoiding any artificial excitation and fully preserving the structure's integrity. In addition to characterizing the dynamic response, the tests served to provide reliable data to update the numerical model of the building. This document describes the methods, instrumentation, and results of both site tests. It also includes a comparison between experimental observations and numerical predictions, contributing to the validation of FREEDAM connections in a realistic seismic-resistant building and supporting their broader implementation in future structural applications.

# 2. Description of the seismic sensor and the standalone monitoring solution

The seismic monitoring system adopted in this study represents a highly innovative solution tailored for high-resolution, output-only dynamic characterization of structures. At its core lies a broadband

monolithic mechanical seismometer, the SE-10HL model, developed by Advanced Scientific Sensors and Systems (Adv3S™). Unlike conventional accelerometers, this sensor operates in an open-loop configuration, directly measuring displacements across a wide frequency range with exceptional sensitivity and minimal noise. Consequently, this solution does not require the adoption of an artificial vibration signal input, allowing to use the environmental vibrations as natural sources for the structural excitation.

The SE-10HL is based on a mechanical oscillator of the GK19A type, exploiting a Watt's Linkage design that ensures highly linear and unidirectional motion of the sensing mass. Displacement is transduced into an electrical signal via a high-resolution Linear Variable Differential Transformer (LVDT). Specifically, the LVDT is the model MHR-010 produced by Measurement Specialities Inc., achieving spectral sensitivities better than  $10^{-8}$  m/ $\sqrt{\text{Hz}}$  between 3.5 Hz and 100 Hz. This configuration allows the sensor to operate effectively from near-static conditions (DC) up to high frequencies, with a nominal natural frequency of 3.80 Hz ±10%. The device is capable of detecting mass displacements within ±0.8 mm and provides a differential analog output of ±10 V, powered by a symmetrical ±18–30 V supply. Its mechanical and electronic stability across a wide thermal range (-40 °C to +85 °C) further enhances its applicability in real-world monitoring.

One of the sensor's distinguishing features is its scalability and modularity. The system architecture allows for future integration with ultra-high-resolution readout technologies, such as optical or interferometric sensors, enabling even greater sensitivity — up to two or three orders of magnitude beyond the current configuration — for demanding applications requiring extremely low noise floors.

This seismometer is integrated into a standalone, portable monitoring system designed to perform long-duration, high-fidelity structural measurements with low energy consumption and minimal installation complexity. Data acquisition is managed by a 24-bit National Instruments™ FieldDAQ FD-11603, which supports simultaneous sampling of eight galvanically isolated channels at rates up to 102.4 kSamples/s. Pre-filtering and delta-sigma ADCs ensure high precision and robust performance under variable environmental conditions. Data is streamed via Ethernet to a control workstation equipped with a custom user interface (Supervisor), which manages acquisition, storage, and synchronization. The system supports the integration of up to 120 sensors of various types (seismic, magnetic, environmental, etc.), offering high versatility for structural monitoring campaigns.

What makes this instrumentation particularly unique is the combination of high displacement sensitivity, broadband frequency response, and non-invasiveness, which allows for reliable detection of subtle structural deformations and resonances without requiring any artificial excitation. This makes it exceptionally suitable for the empirical validation of finite element models, especially in innovative structural typologies such as FREEDAM-equipped steel frames, where capturing realistic boundary conditions and damping behavior is critical. The high signal-to-noise ratio in the low-frequency domain and the ability to measure absolute displacements — rather than inferred accelerations — represent a fundamental advantage when assessing the dynamic performance of full-scale buildings under ambient excitation.

The adopted instrumentation departs from traditional structural testing paradigms. It leverages advanced inertial sensing to provide an accurate, high-resolution, and field-deployable solution aligned with the experimental character of next-generation seismic-resistant constructions. Its application to the DREAMERS demonstrator structure exemplifies how novel sensor technologies can elevate the quality and scope of dynamic assessment in structural engineering.

#### 3. Measurement setup and sensor placement

The experimental vibration monitoring of the C3 building was carried out in two distinct campaigns, corresponding to different construction phases and instrumental configurations. In both cases, the adopted methodology was based on output-only measurements, relying on ambient excitations and high-sensitivity broadband seismometers arranged in configurations tailored to capture the dominant structural response modes.

### 3.1 First monitoring campaign – October 12, 2024

The first test was performed when the structure was in an intermediate state of construction, with the steel frame and composite floor slabs already completed, but no partitions, façades, or technical installations in place. The monitoring system was deployed exclusively at the first-floor level, where six broadband monolithic seismometers were installed. These sensors were arranged in three pairs along the diagonal axis of the floor plan (see Figure 1), allowing for an effective acquisition of modal response data along both the longitudinal and transverse directions.

#### More precisely:

- Odd-numbered channels (CH1, CH3, CH5) were oriented along the transverse (shorter) direction
  of the building.
- Even-numbered channels (CH2, CH4, CH6) were aligned with the longitudinal (longer) direction. All sensors were oriented consistently, with their directional sensitivity axes aligned with the global reference system adopted in the numerical model. This configuration ensured coherent phase information and accurate estimation of mode shapes. Each seismometer was positioned on a rigid stone base to ensure optimal mechanical coupling and to minimize local noise due to microvibrations or substrate irregularities (Figure 2 and Figure 3).

Given the high sensitivity of the adopted sensors, no instrumentation was required on the second floor or the roof. The low-frequency displacement data acquired at the first level proved sufficient to characterize the global dynamic behavior of the structure, including contributions from the upper storeys. Moreover, no sensors were placed on the staircase-elevator core, as it was conceived as a structurally independent element not directly contributing to the global dynamic response of the moment-resisting frame.

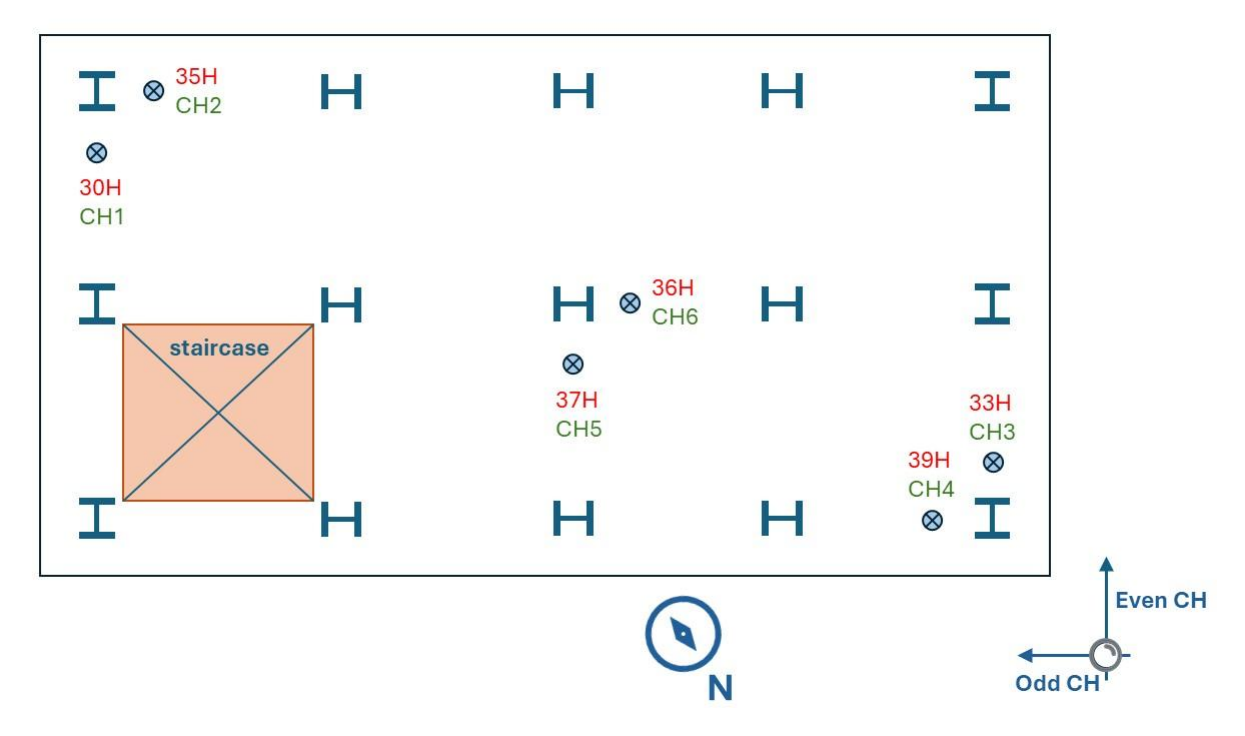


Figure 1. Plan positioning of the sensors in the first campaign of October 12, 2024

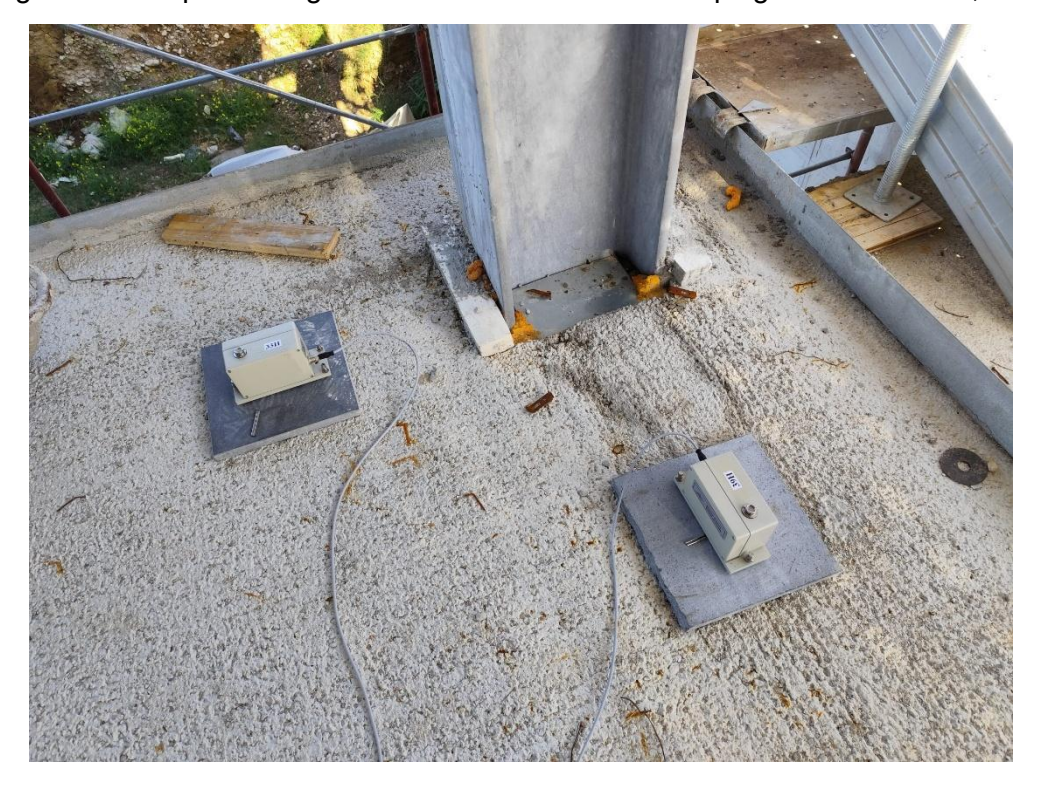


Figure 2. Sensors 33H and 39H in the lower right corner of the building with reference to Figure 1



Figure 3. Sensors 30H and 35H in the lower right corner of the building with reference to Figure 1

# 3.2 Second monitoring campaign – June 7, 2025

The second monitoring session was conducted when the building was in an advanced state of completion, with façades, internal partitions, services, and non-structural elements fully installed. To account for the presence of additional mass and potential interaction between structural and non-structural components, the instrumentation layout was expanded.

As in the first campaign, six sensors were placed at the first-floor level along the same diagonal axes and with identical orientation and coupling procedures as reported in Figure 4. Additionally, a new sensor pair was installed directly on the intermediate landing of the staircase-elevator core, in order to:

- assess potential dynamic interaction between the independent stair structure and the main steel frame;
- capture any local resonance phenomena or secondary modes introduced by the increased mass and stiffness of the completed structure.

However, these data have not been included in the following.

The sensors have been directly located on the floor as reported in Figure 5 and Figure 6.

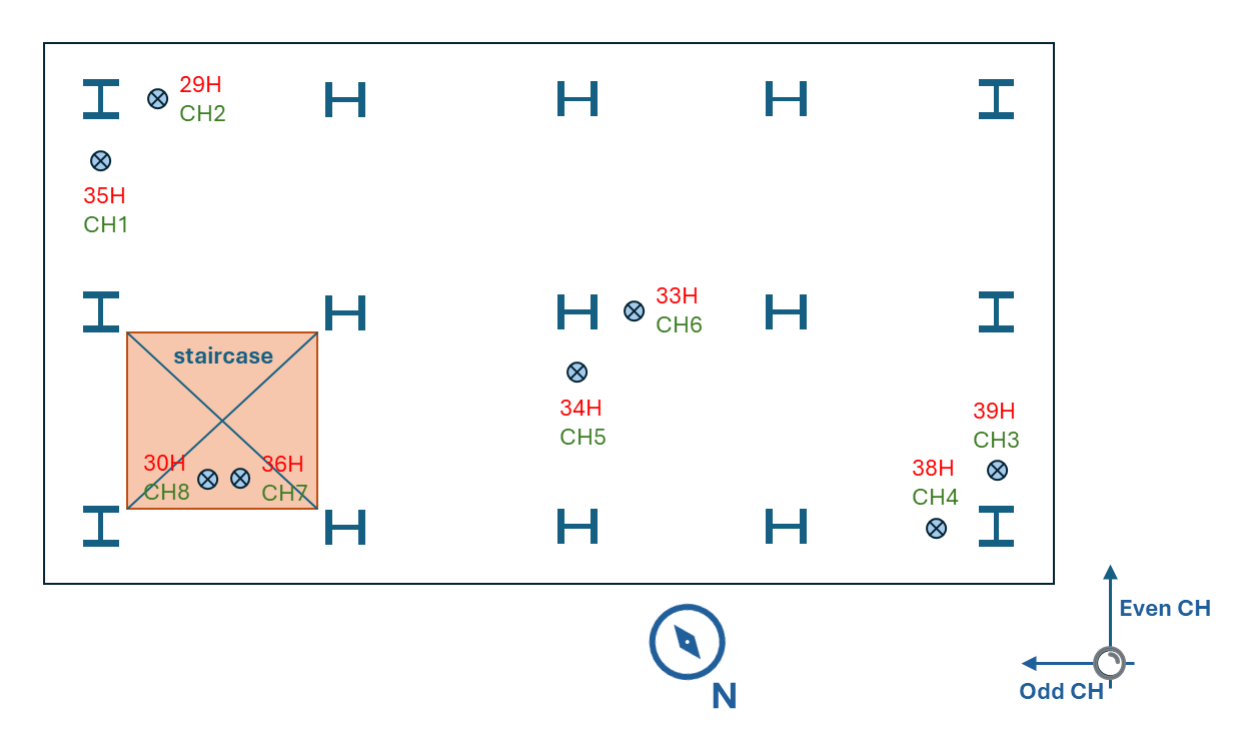


Figure 4. Plan positioning of the sensors in the second campaign of June 07, 2025



Figure 5. Sensors 29H and 35H in the high left corner of the building with reference to Figure 4



Figure 6. Sensors 34H and 33H in the middle of the building with reference to Figure 4

#### 4. Signal acquisition and spectral processing

The broadband mechanical seismometers employed in the monitoring campaigns provided direct analog voltage outputs proportional to absolute displacement. These signals, characterized by a high signal-to-noise ratio even in the low-frequency band, were continuously acquired and digitized at a sampling rate of 5 kHz using a 24-bit resolution data acquisition system. The raw data were stored in uncompressed binary format to preserve the full dynamic range and temporal integrity of the measurements.

To interpret the structural response, the time-domain signals were post-processed along two complementary analytical paths. Firstly, the displacement time histories were examined directly to assess the temporal evolution of structural oscillations, drift phenomena, and transient events. These representations offered insight into the amplitude, phase, and damping behavior of the monitored points. The acquisition of the first and second campaign are reported in Figure 7 and Figure 8, respectively, in terms of translational displacement.

The recorded signals were transformed into the frequency domain through the application of the Fast Fourier Transform (FFT) algorithm. This step allowed the decomposition of the complex structural response into its constituent harmonic components, providing a powerful tool for identifying the dominant natural frequencies and modal content of the structure. Spectral analysis was performed on sliding time windows to generate frequency—time representations (spectrograms), which enabled the tracking of modal energy concentration over time and the detection of possible frequency shifts due to temporary or permanent changes in boundary conditions, mass distribution, or external excitations. The spectrograms for the first and second campaign are reported in Figure 9 and Figure 10.

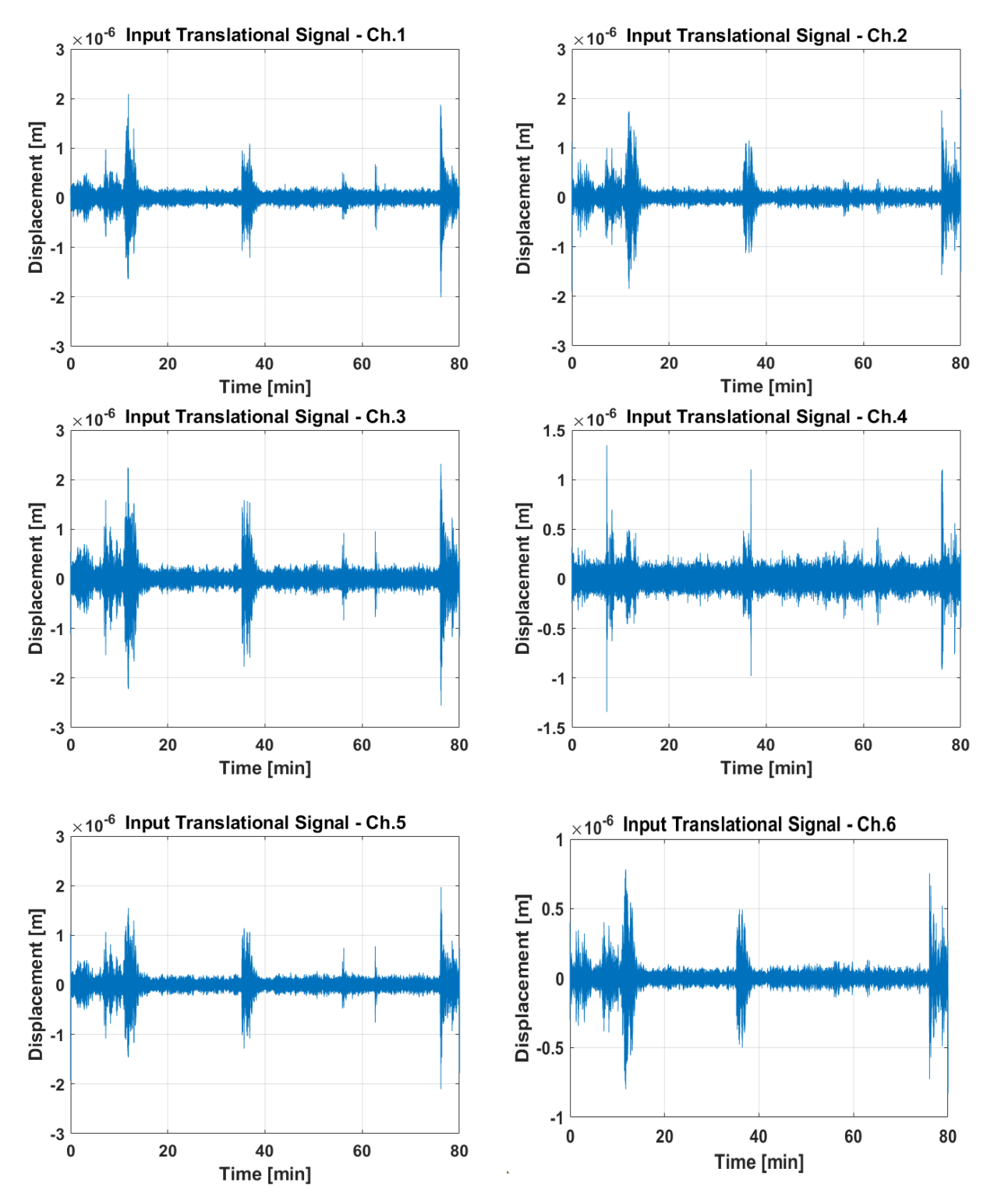


Figure 7. Translational displacement signals recorded during the first campaign in the points of Figure 1.

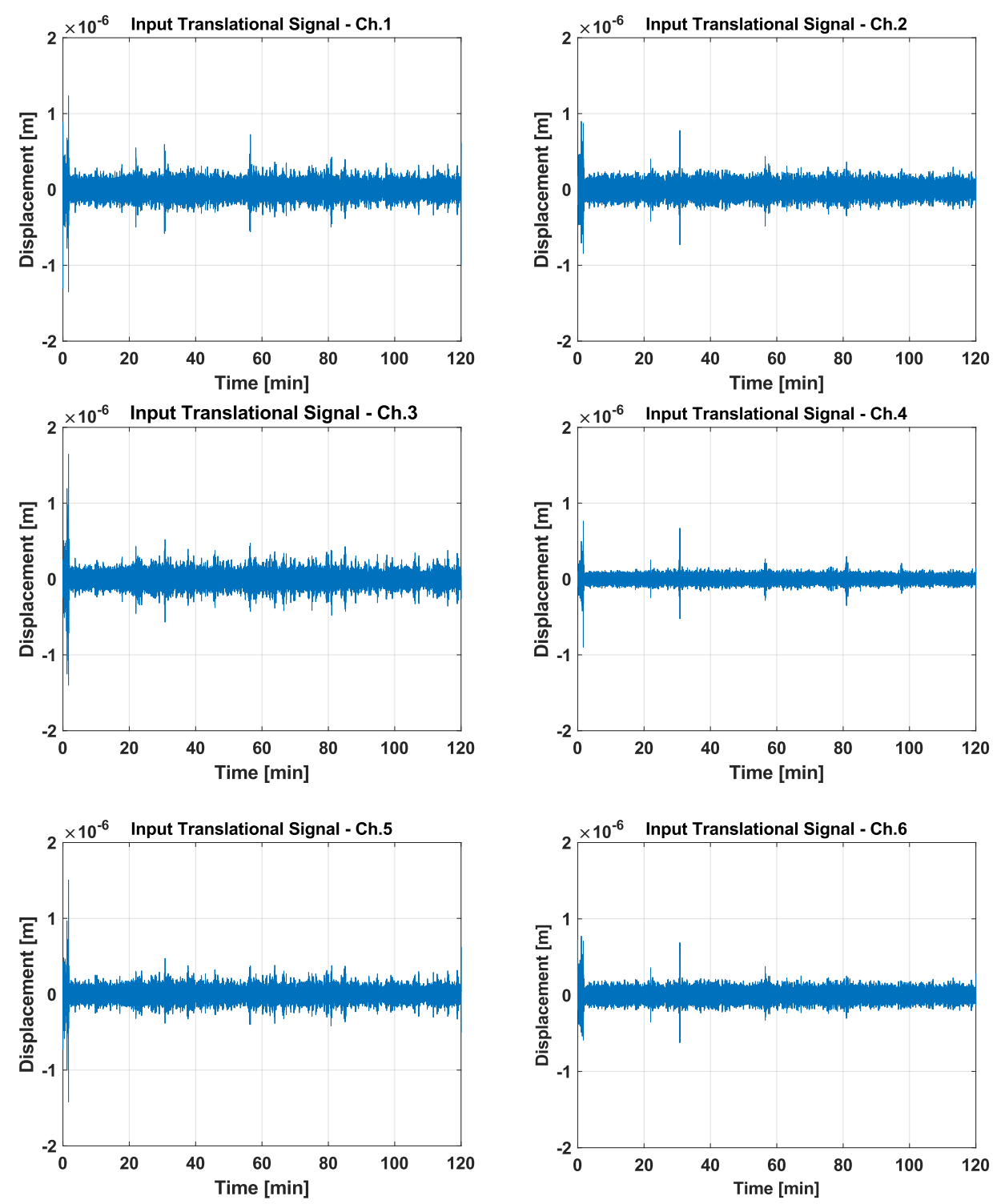


Figure 8. Translational displacement signals recorded during the second campaign in the points of Figure 4.

The FFT-based analysis was conducted with appropriate windowing (e.g., Hanning windows) and zero-padding strategies to improve frequency resolution and minimize spectral leakage. Importantly, the ability of the seismometers to provide true displacement measurements, rather than acceleration-derived displacements, ensured that the spectral content in the low-frequency band (1–10 Hz) was preserved with high fidelity, avoiding the distortions typically introduced by numerical double integration of acceleration signals. This property was essential for the accurate identification of the

fundamental structural modes, which, in the case of the C3 building, fall within a relatively low frequency range due to the structural typology and material configuration.

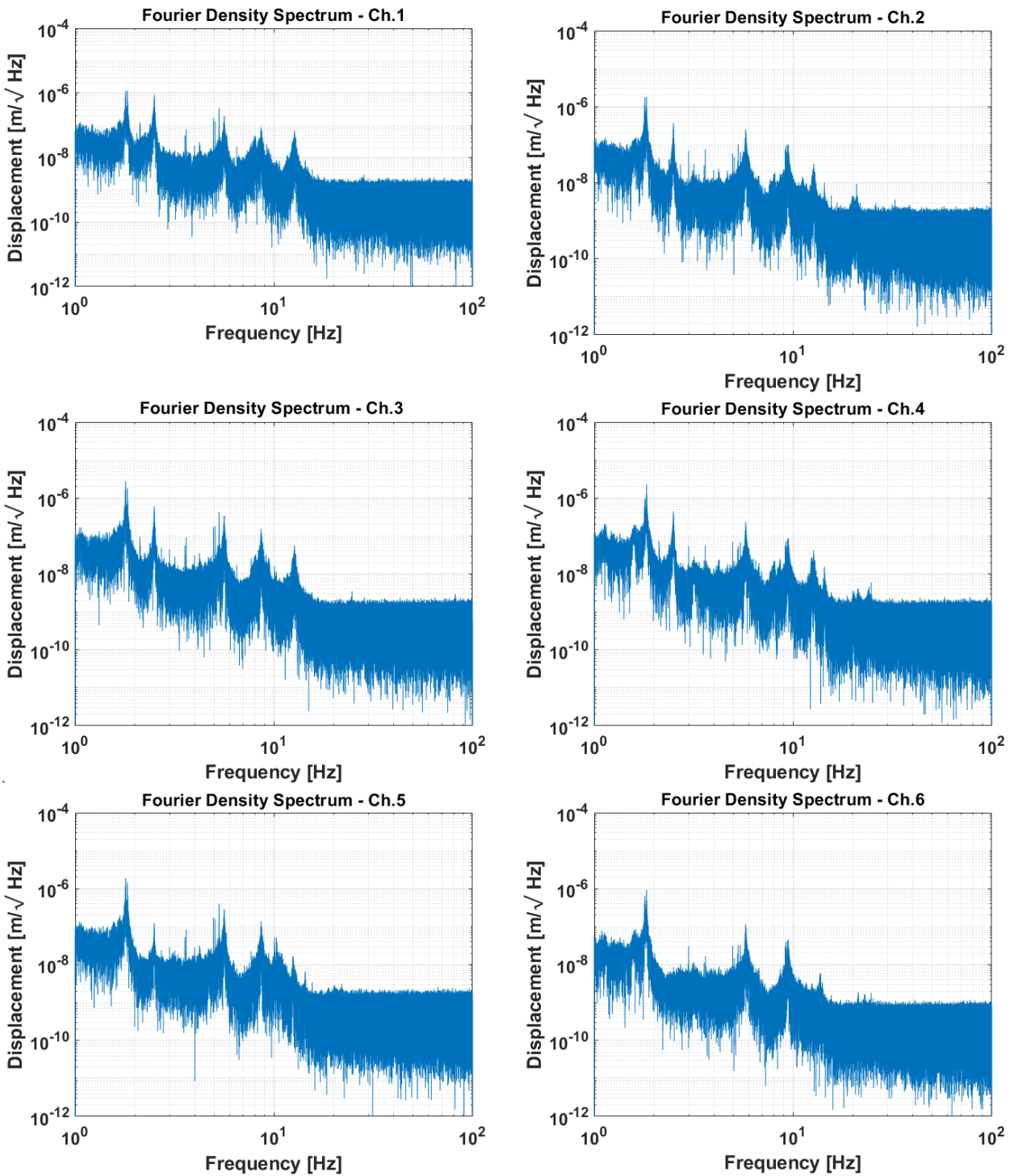
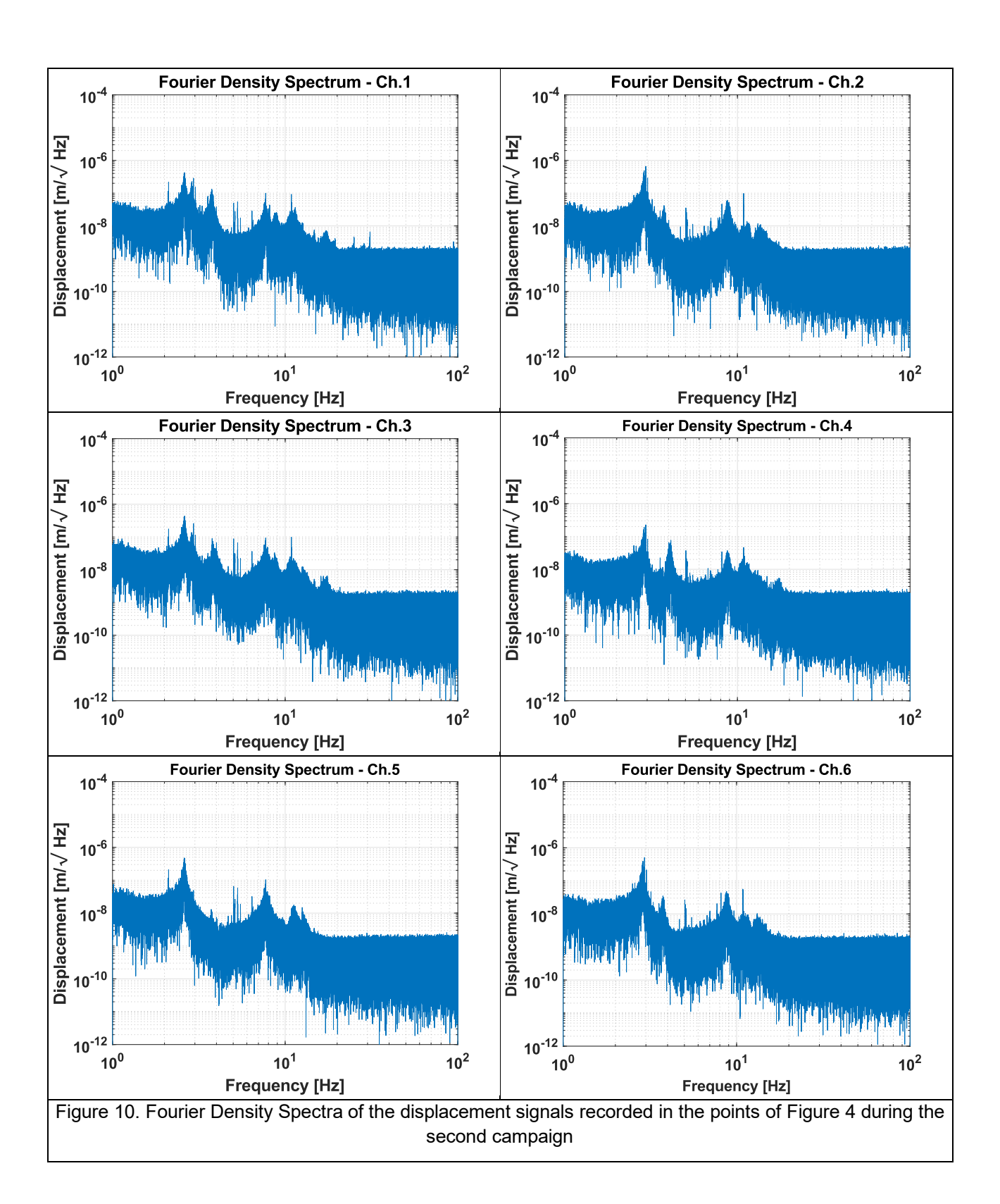


Figure 9. Fourier Density Spectra of the displacement signals recorded in the points of Figure 1 during the first campaign



# 5. Operational modal analysis results

To identify the dynamic properties of the C3 building under operational conditions — that is, in the absence of controlled excitation — the experimental data acquired during the dynamic identification campaigns were processed using Operational Modal Analysis (OMA) techniques. Unlike Experimental Modal Analysis (EMA), which relies on known input forces, OMA operates solely on

the system's response to ambient excitations, such as wind, microtremors, and human activity. This approach is particularly suitable for in-situ monitoring of full-scale structures, where artificial excitation may be impractical, invasive, or undesirable.

The analysis was conducted by interpreting the displacement time histories recorded by the broadband seismometers. These signals were pre-processed to remove low-frequency trends (e.g., thermal drift, settlement effects) and high-frequency noise through band-pass filtering. Once the signals were conditioned, OMA algorithms were applied to extract the system's modal characteristics. Among the various available techniques, the method adopted in this study was the Stochastic Subspace Identification with Covariance-driven formulation (SSI-COV), which is widely recognized for its robustness in extracting stable modal parameters from ambient vibration data.

The SSI-COV algorithm relies on the state-space representation of the dynamic system and operates by computing the output covariance matrices over a finite number of time lags. These matrices are used to construct a block Hankel matrix, from which a stochastic realization of the system is obtained through singular value decomposition (SVD). The state matrices derived from this process yield the system poles, from which natural frequencies and damping ratios can be directly computed. The associated mode shapes are extracted as the dominant directions of motion at each instrumented node and are expressed in relative amplitude and phase.

To ensure the reliability of the identified modes, the procedure was repeated over multiple data segments, and the results were filtered using a stabilization diagram. This diagram displays the estimated modal parameters as a function of the model order, allowing the user to distinguish physical modes — which remain consistent across orders — from spurious numerical artefacts. Only modes exhibiting stable frequency, damping, and mode shape across increasing model orders were retained for interpretation and comparison with numerical predictions.

The natural frequencies extracted from the OMA ranged, in both campaigns, from approximately 1.1 Hz to 20 Hz, capturing both fundamental translational modes and higher-order bending or torsional components. The damping ratios identified from the logarithmic decrement of the modal responses were generally low, as expected for steel-frame structures with bolted connections. However, differences between the first and second campaigns were observed, particularly due to the addition of non-structural elements such as finishings and façades, which introduced additional damping mechanisms and mass contributions. In the second campaign, the damping ratio increased confirming the influence of partitions and architectural finishes on energy dissipation.

By relying on high-quality displacement data and advanced stochastic identification techniques, the adopted OMA framework allowed for the accurate and non-invasive characterization of the dynamic behavior of the building, providing a crucial experimental benchmark for the calibration of the FEM models developed in the DREAMERS project. This also demonstrates the feasibility and efficacy of using ambient vibration testing in conjunction with innovative sensing systems for structural health assessment in complex building systems.

Following the identification of the modes, a Modal Assurance Criterion (MAC) analysis was conducted to quantify the consistency and orthogonality of the extracted mode shapes. The MAC is a statistical indicator that evaluates the degree of linear correlation between two modal vectors. Values close to unity (MAC  $\approx$  1.0) indicate a strong agreement, while lower values reveal inconsistencies due to noise, mode mixing, or numerical artefacts. In this study, the MAC was used to:

Verify the internal consistency of the mode shapes extracted from different time segments;

- Compare mode shapes between the two monitoring campaigns;
- Assess the correlation between experimental and numerical mode shapes derived from FEM simulations.

The resulting MAC matrix confirmed a high degree of repeatability for the fundamental modes across the two test campaigns and provided valuable guidance for the iterative calibration of the numerical model, particularly in the presence of evolving boundary conditions and non-structural elements.

By relying on high-quality displacement data, advanced stochastic identification algorithms, and rigorous correlation metrics such as the MAC, the adopted OMA framework allowed for the accurate and non-invasive characterization of the dynamic behaviour of the building. These results serve as a reliable benchmark for validating the numerical simulations and for tracking potential deviations in structural performance over time within the DREAMERS project.

#### 6. FEM Modal Analysis

The numerical modal analysis of the building was performed using the finite element software SAP2000. Structural members, such as beams and columns, were modelled as beam-column elements considering an infinite stiffness of the panel zone. The columns are considered as fixed at the level of the first floor neglecting the portion of the columns embedded within the reinforced concrete foundation blocks.

The floor system was represented using shell elements, with loads assumed to act in the actual load-transfer direction of the slab. The real thickness of the composite floor slab was accounted for in the shell modelling, ensuring accurate representation of both stiffness and mass. The in-plane stiffness of the slab was idealized by assigning rigid diaphragm constraints at the floor level. Additionally, the presence and exact location of openings - such as service shafts and the staircase core - were carefully modelled, as these discontinuities influence both the local and global dynamic properties of the structure as well as the mass distribution. The material properties used in the numerical model included an elastic modulus of steel equal to 210000 MPa, a unit weight of steel of 77 kN/m³, and a unit weight of concrete of 25 kN/m³. Furthermore, a line load of 4.5 kN/m was applied to simulate the effect of the roof-level concrete parapets.

The main results for the structural frame configuration corresponding to the monitoring campaign of October 12, 2024, are presented in Figure 11, showing the displacement contours associated with the first three vibration modes. Furthermore, Table 1 provides a comparison between the experimentally identified modes and those derived from the finite element model, including the corresponding discrepancies. It is observed that not all the modes identified by the measure campaign have their correspondence in the modal analysis results developed by FEM. In fact, the OMA based on experimental measures supports the identification of structural vibration modes together with the excitatory modes depending on environmental forcings. Conversely, the modal analysis relying on the FEM simulations of a structure, represented as an individual multi-material object, depending also on an accurate representation of all the structural components and their mechanical behavior, represents only the vibration modes of the structure alone.

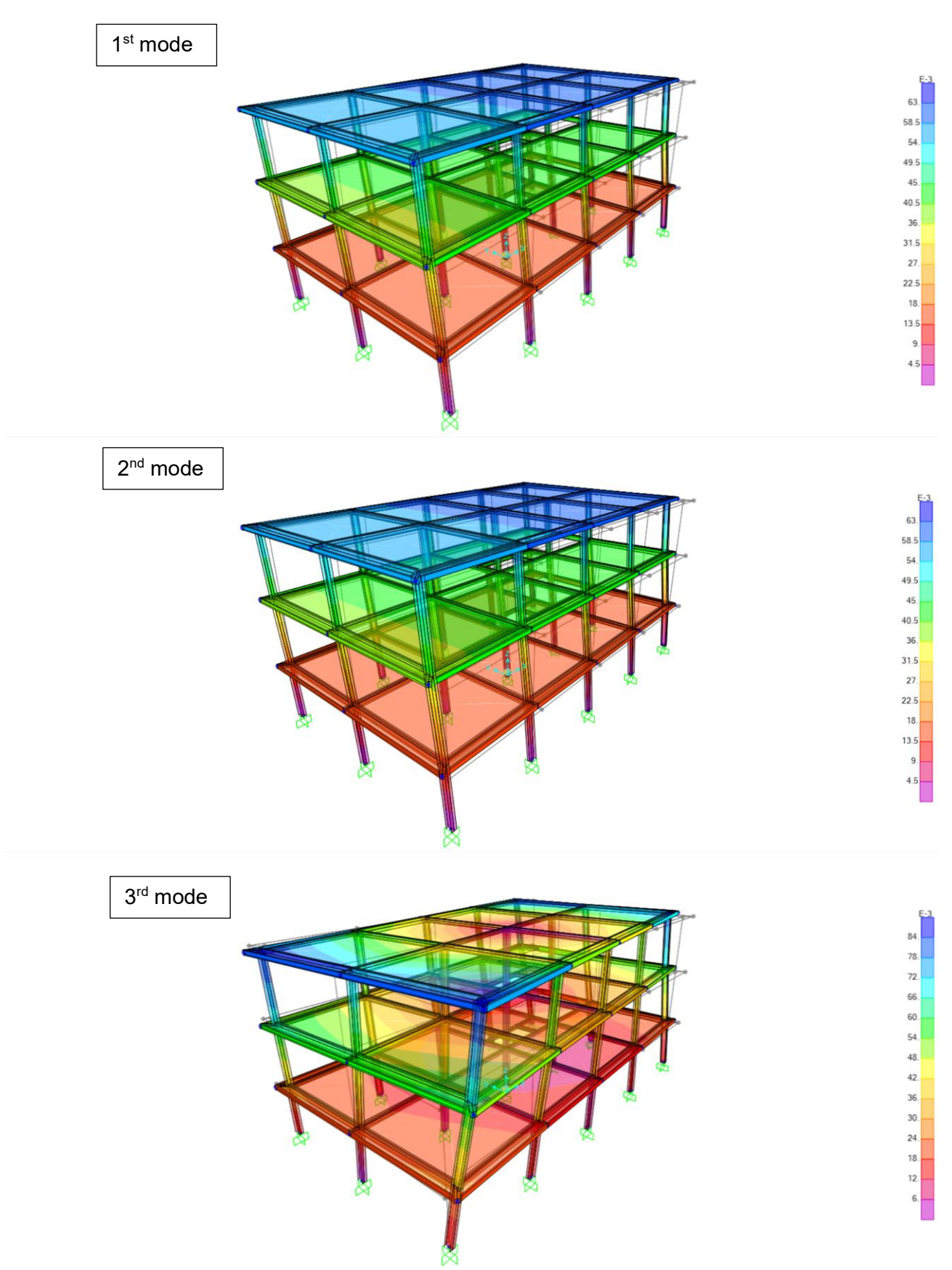


Figure 11. Modal analysis contours for the FEM simulations of the building in the configuration of the first campaign of October 12, 2024.

Table 1. Comparison in terms of periods and frequencies between FEM simulations by SAP2000 and measures with reference to the first campaign of dynamic identification (October 12, 2024).

	SAP 2000		MEASURES			
Mode	T (s)	f (Hz)	T (s)	f (Hz)	Damping (%)	Error (%)
1	0.565	1.771	0.561	1.783	0.09	-0.69%
2	0.486	2.059	0.510	1.959	1.43	5.09%
3	0.401	2.496	0.401	2.496	0.22	0.01%
4	0.183	5.466	0.184	5.424	0.01	0.78%
6	0.133	7.507	0.128	7.788	0.12	-3.61%
7	0.118	8.440	0.122	8.175	0.12	3.24%
8	0.104	9.615	0.103	9.728	0.26	-1.16%
9	0.098	10.245	0.097	10.303	0.06	-0.56%
10	0.095	10.479	0.094	10.663	0.25	-1.72%
11	0.090	11.169	0.087	11.528	0.24	-3.11%

The finite element model corresponding to the C3 building in the second monitoring campaign also accounts for the permanent non-structural loads acting at the floor levels, including: the internal finishing and partition walls (equal to 1.85 kN/m² and 2.20 kN/m²), the brise-soleil system (0.15 kN/m²), the solar panels installed on the top floor (0.10 kN/m²), heavy mechanical systems (0.75 kN/m²), and the external walls (4.5 kN/m²). The main results for the structural frame configuration corresponding to the monitoring campaign of June 07, 2025, are presented in Figure 12, showing the displacement contours associated with the first three vibration modes. Furthermore, Table 2 provides a comparison between the experimentally identified modes and those derived from the finite element model, including the corresponding discrepancies.

Also in this case, several modes identified through the experimental measurement campaign do not find a direct counterpart in the results of the numerical modal analysis performed via FEM simulations. This discrepancy arises from the fact that the experimental OMA approach captures not only the intrinsic structural vibration modes, but also modes influenced by environmental excitations, such as seismic inputs, winds, or vibrations of anthropic origin. On the other hand, the FEM-based modal analysis, which models the structure as a separate and discrete multi-material system with a given geometry, can reproduce only the pure structural modes, eventually implemented with the representation soil-structure interactions, provided that all elements and their material behaviour are accurately defined. As a result, the resulting simulations reflect solely the expected dynamic characteristics of the structure, whereas the experimental analysis incorporates a broader range of real-world dynamic responses.

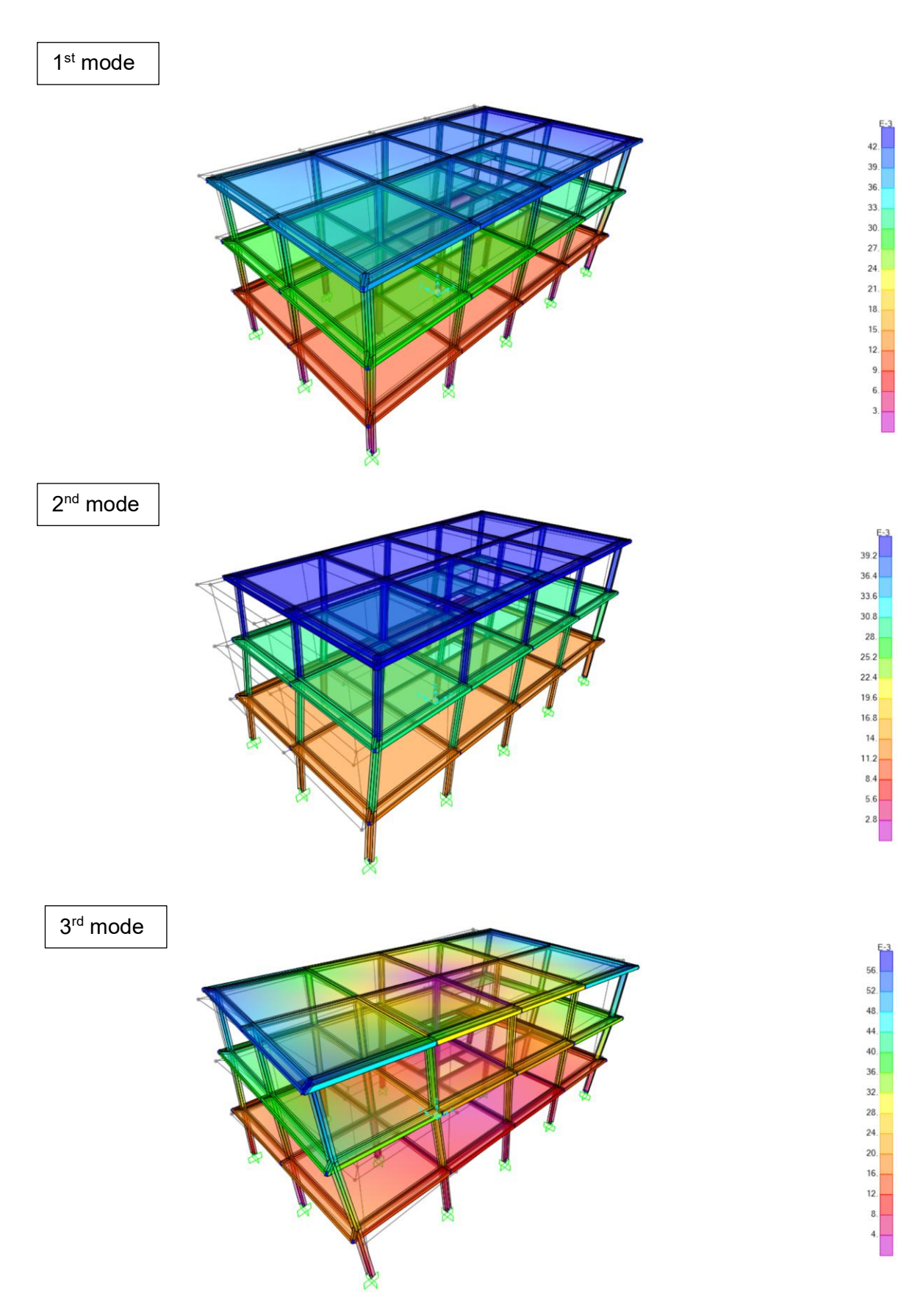


Figure 12. Modal analysis contours for the FEM simulations of the building in the configuration of the second campaign of June 07, 2025.

Table 2. Comparison in terms of periods and frequencies between FEM simulations by SAP2000 and measures with reference to the second campaign of dynamic identification (June 07, 2025)

SAP 2000			MEASURES				
Mode	T (s)	f (Hz)	T (s)	f (Hz)	Damping (%)	Error (%)	
1	0.825103	1.21197	0.834	1.199	4.3	-1.07%	
3	0.609278	1.641286	0.59	1.695	1.47	3.27%	
4	0.27868	3.588351	0.284	3.525	0.12	-1.77%	
5	0.242029	4.131736	0.242	4.131	0.25	-0.02%	
6	0.212196	4.712622	0.234	4.268	0.7	-9.43%	
9	0.16355	6.11435	0.16	6.242	0.51	2.09%	
12	0.102728	9.734443	0.104	9.608	0.83	-1.30%	

#### 7. Conclusions

The dynamic identification of the C3 demonstration building was conceived as a fundamental step in the experimental validation of its seismic performance, with particular attention to the behavior of the FREEDAM connection system and the structural evolution throughout the construction process. The adoption of this methodology allowed for the characterization of the building's dynamic properties in two distinct stages: an intermediate phase during construction (October 2024) and a near-completion phase (June 2025), thereby providing a comprehensive assessment of the structural response under real boundary conditions.

To ensure high-resolution, displacement-based measurement of ambient vibrations, the monitoring campaigns employed broadband mechanical seismometers specifically designed for low-frequency structural dynamics. These sensors, integrated into a modular and portable standalone acquisition system, enabled accurate detection of small-amplitude vibrations without the need for artificial excitation sources. The data acquisition was performed in multiple channels with directional sensitivity, allowing for full spatial resolution of the modal response.

The recorded displacement signals were processed using Operational Modal Analysis (OMA) techniques, with the Stochastic Subspace Identification - Covariance-driven (SSI-COV) algorithm selected for its robustness in extracting stable modal parameters from ambient data. The consistency of identified modes was validated through the Modal Assurance Criterion (MAC), which confirmed the reliability of the extracted mode shapes and enabled meaningful comparison across campaigns and with numerical predictions.

The analysis revealed a stable set of vibration modes, with natural frequencies ranging from approximately 1.2 Hz to 6.5 Hz in both campaigns. A total of 10 dominant modes were clearly identified in the first test campaign and 7 in the second, indicating improved resolution of the measurement system and the high match with the expected modal behaviour derived from the FEM simulations.

A comparison of the modal damping ratios, as summarized in Table 1 (October 2024) and Table 2 (June 2025), highlights a measurable increase in energy dissipation with the progression of construction. This increase is attributable to the added mass and interaction effects introduced by non-structural elements such as partition walls, brise-soleil systems, mechanical installations, and

façades, which enhance frictional and hysteretic dissipation mechanisms, not present in the bare structural frame.

In conclusion, the integrated experimental framework — combining high-sensitivity instrumentation, advanced OMA algorithms, and multistage field testing — proved effective in capturing the dynamic evolution of the C3 building. The results underscore the influence of non-structural components on modal characteristics and confirm the potential of this methodology for performance-based validation of innovative seismic-resistant structures. The outcomes will inform the updating and calibration of the numerical models developed within the project and support future design optimization and monitoring strategies.

#### 8. References

- [1] Altunisik, A.C., Bayraktar, A., Ozdemir, H., 2012. Seismic safety assessment of eynel highway steel bridge using ambient vibration measurements. Smart Structures and Systems 10, 131–154. https://doi.org/10.12989/SSS.2012.10.2.131
- [2] Benevicius, V., Ostasevicius, V., Gaidys, R., 2013. Identification of Capacitive MEMS Accelerometer Structure Parameters for Human Body Dynamics Measurements. Sensors 13, 11184–11195. https://doi.org/10.3390/s130911184
- [3] Chai, S., Wang, S., Liu, C., Liu, X., Liu, T., Yang, R., 2024. A visual measurement algorithm for vibration displacement of rotating body using semantic segmentation network. Expert Systems with Applications 237, 121306. https://doi.org/10.1016/j.eswa.2023.121306
- [4] Chen, J., Chen, X., Liu, W., 2014. Complete Inverse Method Using Ant Colony Optimization Algorithm for Structural Parameters and Excitation Identification from Output Only Measurements. Mathematical Problems in Engineering 2014, 185487. https://doi.org/10.1155/2014/185487
- [5] Collette, C., Janssens, S., Fernandez-Carmona, P., Artoos, K., Guinchard, M., Hauviller, C., Preumont, A., 2012. Review: Inertial Sensors for Low-Frequency Seismic Vibration Measurement. Bulletin of the Seismological Society of America 102, 1289–1300. https://doi.org/10.1785/0120110223
- [6] Dang, H., Nguyen, T.-T., 2023. Robust Vibration Output-only Structural Health Monitoring Framework Based on Multi-modal Feature Fusion and Self-learning. Period. Polytech. Civil Eng. https://doi.org/10.3311/PPci.21756
- [7] D'Emilia, G., Gaspari, A., Natale, E., 2019. Amplitude–phase calibration of tri-axial accelerometers in the low-frequency range by a LDV. J. Sens. Sens. Syst. 8, 223–231. https://doi.org/10.5194/jsss-8-223-2019
- [8] Fiorillo, A.S., Critello, C.D., Pullano, S.A., 2018. Theory, technology and applications of piezoresistive sensors: A review. Sensors and Actuators A: Physical 281, 156–175. https://doi.org/10.1016/j.sna.2018.07.006
- [9] Ghemari, Z., Belkhiri, S., Saad, S., 2024. New parameters for the capacitive accelerometer to reduce its measurement error and power consumption. Measurement: Energy 3, 100018. https://doi.org/10.1016/j.meaene.2024.100018

- [10] Gupalov, V., Kukaev, A., Shevchenko, S., Shalymov, E., Venediktov, V., 2018. Physical Principles of a Piezo Accelerometer Sensitive to a Nearly Constant Signal. Sensors 18, 3258. https://doi.org/10.3390/s18103258
- [11] Lignos, D.G., Miranda, E., 2014. Estimation of base motion in instrumented steel buildings using output-only system identification. Earthq Engng Struct Dyn 43, 547–563. https://doi.org/10.1002/eqe.2359
- [12] Peeters, B., De Roeck, G., 1999. Reference-based stochastic subspace identification for output-only modal analysis. Mechanical Systems and Signal Processing 13, 855–878. https://doi.org/10.1006/mssp.1999.1249
- [13] Shangguan, Z., Xing, T., Zhou, S., Ma, S., 2023. Research on full-field vibration displacement measurement based on grid CCD moiré method. Optics Communications 549, 129878. https://doi.org/10.1016/j.optcom.2023.129878
- [14] Shen, H., Zhu, Z., Lu, H., Ju, H., Huang, J., Chen, Z., 2023. Development of a Sandwiched Piezoelectric Accelerometer for Low-Frequency and Wide-Band Seismic Exploration. Sensors 23, 9168. https://doi.org/10.3390/s23229168
- [15] Wu, T., You, D., Gao, H., Lian, P., Ma, W., Zhou, X., Wang, C., Luo, J., Zhang, H., Tan, H., 2023. Research Status and Development Trend of Piezoelectric Accelerometer. Crystals 13, 1363. https://doi.org/10.3390/cryst13091363
- [16] Xu, Y., Zhao, L., Jiang, Z., Ding, J., Xu, T., Zhao, Y., 2016. Analysis and design of a novel piezoresistive accelerometer with axially stressed self-supporting sensing beams. Sensors and Actuators A: Physical 247, 1–11. https://doi.org/10.1016/j.sna.2016.04.053
- [17] Yoder, N.C., Adams, D.E., 2022. Commonly used sensors for civil infrastructures and their associated algorithms, in: Sensor Technologies for Civil Infrastructures. Elsevier, pp. 51–76. https://doi.org/10.1016/B978-0-08-102696-0.00014-2
- [18] Yu, J.-C., Lan, C.-B., 2001. System modeling of microaccelerometer using piezoelectric thin films. Sensors and Actuators A: Physical 88, 178–186. https://doi.org/10.1016/S0924-4247(00)00502-1